

# Structural and electrical behaviour of sol-gel derived Li-Ni-Co ferrite/SiO<sub>2</sub> nanocomposites

Nandeibam Nilima<sup>1</sup>, Mamata Maisnam<sup>2</sup>, Sumitra Phanjoubam<sup>1\*</sup>

<sup>1</sup>Department of Physics, Manipur University, Canchipur, 795003, India

<sup>2</sup>Department of Physics, NIT Manipur, Langol, 795004, India

\*Corresponding author: Tel: (+91)94-36894642; E-mail: sumitraphanjoubam@gmail.com

Received: 31 March 2016, Revised: 26 September 2016 and Accepted: 03 November 2016

DOI: 10.5185/amp.2017/506

www.vbripress.com/amp

## Abstract

Li-Ni-Co ferrite/SiO<sub>2</sub> composites with representative formula Li<sub>0.41</sub>Ni<sub>0.1</sub>Co<sub>0.08</sub>Fe<sub>2.41</sub>O<sub>4+x</sub>SiO<sub>2</sub> (i.e., x = 0wt. %, 5wt. %, 10wt. % and 20wt. %) were prepared by sol-gel method. The prepared composites were pre-sintered at 600°C for 2 hrs and then finally sintered at 1000°C for 6 hrs. X-ray diffraction studies showed diffraction peaks indicating single phase with spinel structure. However, peaks of SiO<sub>2</sub> were found in composites of higher (x). The microstructure of the samples was studied by using Scanning Electron Microscopy. The crystallite size and average grain size were found to decrease with increase of SiO<sub>2</sub> content. The room temperature frequency variation of dielectric constant and dielectric loss was measured from 100Hz-1MHz and they showed a dispersive behavior. The variation has been explained by Verwey mechanism of electron hopping and Koop's two-layer model. The addition of SiO<sub>2</sub> plays significant role in influencing the various structural, microstructural and electrical properties. Uniform and refined microstructures are observed with the addition of SiO<sub>2</sub> and this reduces the value of dielectric constant and loss significantly, which is desirable for high frequency applications. The results obtained and mechanisms involved are discussed. Copyright © 2017 VBRI Press.

**Keywords:** Ferrites, sol-gel, XRD, SEM, dielectric constant.

## Introduction

Magnetic nanoparticles with spinel structure are of great interest due to their potential applications in various technological devices. Lithium and substituted lithium ferrites exhibit favourable properties such as high resistivity, Curie temperature and saturation magnetization, low eddy current losses, stress sensitivity of remanance etc. for use in microwave devices [1-4]. The properties of these ferrites are strongly dependent on various factors like composition, nature and amount of the substituents, process of synthesis, sintering conditions etc. [5, 6]. Substitution of Ni<sup>2+</sup> in Li-ferrites increases the remanance and remanance ratio while substitution of small amount of Co<sup>2+</sup> in Li ferrite increases power handling capacity and coercivity [7, 8]. Recently, nonconventional methods or chemical methods for preparation of lithium ferrites have emerged as a potential option. These methods are relatively simple and less time consuming, while being effective in producing stoichiometric nanosized particles with good homogeneity [9, 10]. Thus, simultaneous substitution of small amount of Ni<sup>2+</sup> and Co<sup>2+</sup> in Li-ferrites and prepared by chemical method is expected to yield interesting properties. Also investigation of Li-ferrites and mixed Li-ferrites prepared in presence of various non-magnetic materials like SiO<sub>2</sub>, V<sub>2</sub>O<sub>5</sub>, PbO, Al<sub>2</sub>O<sub>3</sub>, Bi<sub>2</sub>O<sub>3</sub> etc. to tailor desired structural,

electrical and magnetic properties is a hot topic of research [11-16]. Among them, SiO<sub>2</sub> is an interesting addition [11, 12, 17, 18]. Several workers have reported that the addition of nano-SiO<sub>2</sub> can modify the dielectric as well as magnetic properties of various ferrites. SiO<sub>2</sub> prepared using tetraethylorthosilicate (TEOS) or tetramethoxysilane (TMOS) are expensive and often very toxic [19]. Hence, in the present work nano SiO<sub>2</sub> was synthesized using low cost sodium silicate and hydrochloric acid by co-precipitation method with PVA as dispersion agent. The synthesized SiO<sub>2</sub> was used to prepare Li-Ni-Co ferrite/SiO<sub>2</sub> nanocomposites by sol-gel method. The present paper reports the modification on various structural, microstructural and electrical properties of Li-Ni-Co ferrite/SiO<sub>2</sub> composites due to varying amount of SiO<sub>2</sub>.

## Experimental

### Materials

For preparation of nanosized SiO<sub>2</sub>:

Raw materials used for preparation were polyvinyl alcohol (Loba Chemie, Bombay), hydrochloric acid (LR, 35-38%) and sodium silicate (M.W. 284.20, VEB Research Laboratory, India).

For preparation of Li-Ni-Co ferrite/SiO<sub>2</sub> nanocomposites:

The raw materials for synthesis of Li-Ni-Co ferrite/SiO<sub>2</sub> composites includes lithium nitrate (purity~ 98% Merck, Mumbai), cobalt nitrate (purity~ 99%, Loba Chemie, Bombay), iron (III) nitrate (purity~98% Merck, Mumbai) and Nickel nitrate (purity~97%, Merck India), Ethylene glycol (purity~ 99% Merck, Mumbai), as starting materials.

### Material synthesis

Nano-SiO<sub>2</sub> was successfully synthesized by acid hydrolysis of sodium silicate using dilute hydrochloric acid. 15% sodium silicate solution was prepared with 1% polyvinyl alcohol solution. The solution was heated at 60 °C with constant stirring, then 0.5N HCl was added to it slowly to maintain the pH of the mixture between 1 and 2. At this pH, the solution was kept for 30 mins maintaining the same temperature to carry out acid hydrolysis of sodium silicate. The mixture was then washed thoroughly with distilled water in order to remove all the sodium chloride which have been formed and finally kept at 50 °C till the mixture dried [20].

Li-Ni-Co ferrite/SiO<sub>2</sub> composites with representative formula Li<sub>0.41</sub>Ni<sub>0.1</sub>Co<sub>0.08</sub>Fe<sub>2.41</sub>O<sub>4</sub> + xSiO<sub>2</sub> (i.e., x = 0wt. %, 5wt. %, 10wt. % and 20wt. %) were prepared by chemical sol-gel method. Stoichiometric amount of Fe(NO<sub>3</sub>)<sub>3</sub>.6H<sub>2</sub>O, LiNO<sub>3</sub>.3H<sub>2</sub>O, Ni(NO<sub>3</sub>)<sub>2</sub>.6H<sub>2</sub>O and Co(NO<sub>3</sub>)<sub>2</sub>.6H<sub>2</sub>O were dissolved in ethylene glycol in the molar ratio 3:1 and required amount of SiO<sub>2</sub> was added into the mixture and heated at 40 °C to get a homogeneous clear solution. The temperature was raised to 80 °C for 20 min to get a wet gel. Then raising the temperature to 130 °C, the gel gets dried after which it gets self-ignited giving a highly voluminous fluffy product. The powder so obtained is the desired nanocomposite. The as-prepared composite powder was presintered at 600 °C for 2 hrs. Then the calcined powder obtained was mixed with a small amount of PVA (3% by weight) and pressed in the form of pellet by applying a load of 100Kg/cm<sup>2</sup> for 5 min. The samples were then heated at 1000 °C for 6 hours in air and subsequently furnace cooled.

### Characterizations

XRD studies were carried out on the samples using Phillips X-Pert Pro PAN analytical X-ray diffractometer using Cu-Kα radiation whose wavelength, λ is 1.54Å. From the XRD data, the lattice constant, 'a' was calculated using the relation:

$$d = a / (h^2 + k^2 + l^2)^{1/2}. \quad (1)$$

The crystallite size of the particles was determined from XRD data using the Scherrer formula,

$$D = 0.94 \lambda / \beta \cos \theta, \quad (2)$$

where, D is the crystallite size, λ the wavelength of Cu-Kα radiation, β the full width at half maximum and θ the Bragg angle. Electrical contacts were made on both the flat surfaces of the pellets using silver coating. The dielectric measurements were carried out on these electroded pellets using an Aligent HP 4284 A LCR meter from 100Hz to 1MHz. The microstructure of the samples was studied by using a Scanning Electron Microscopy (SEM FEI QUANTA-250).

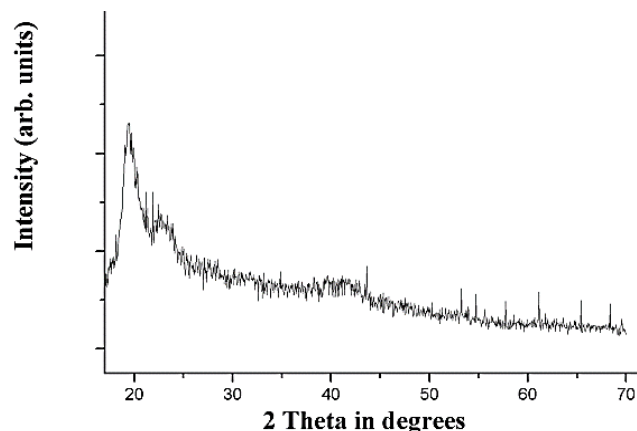


Fig. 1. XRD patterns for as-prepared SiO<sub>2</sub>.

### Results and discussion

Fig. 1 shows the XRD pattern of the as-prepared SiO<sub>2</sub> and a broad band centered about ~ 2θ=20° is observed indicating the amorphous SiO<sub>2</sub> phase [21]. The XRD patterns for the Li-Ni-Co ferrite/SiO<sub>2</sub> composites are depicted in Fig. 2, showing intense diffraction peaks at specific angles corresponding to planes namely (220), (311), (400), (422), (511), (440) showing single phase spinel structure of the ferrite materials in the composites. The patterns also showed peaks at 2θ = 31°, 41°, 49° and 64° marked with \* due to SiO<sub>2</sub> crystallites which have been formed after sintering. The observed peak at 33° in the figure may be due to the α-Fe<sub>2</sub>O<sub>3</sub> which may have formed due to the preferential loss of one or more of the divalent cation during sintering [22].

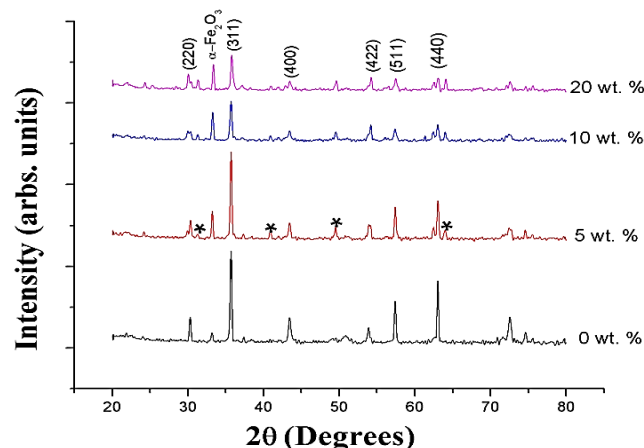


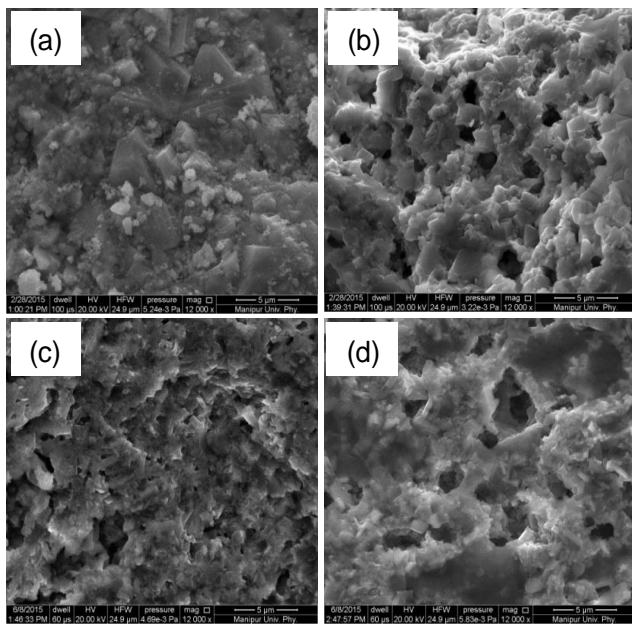
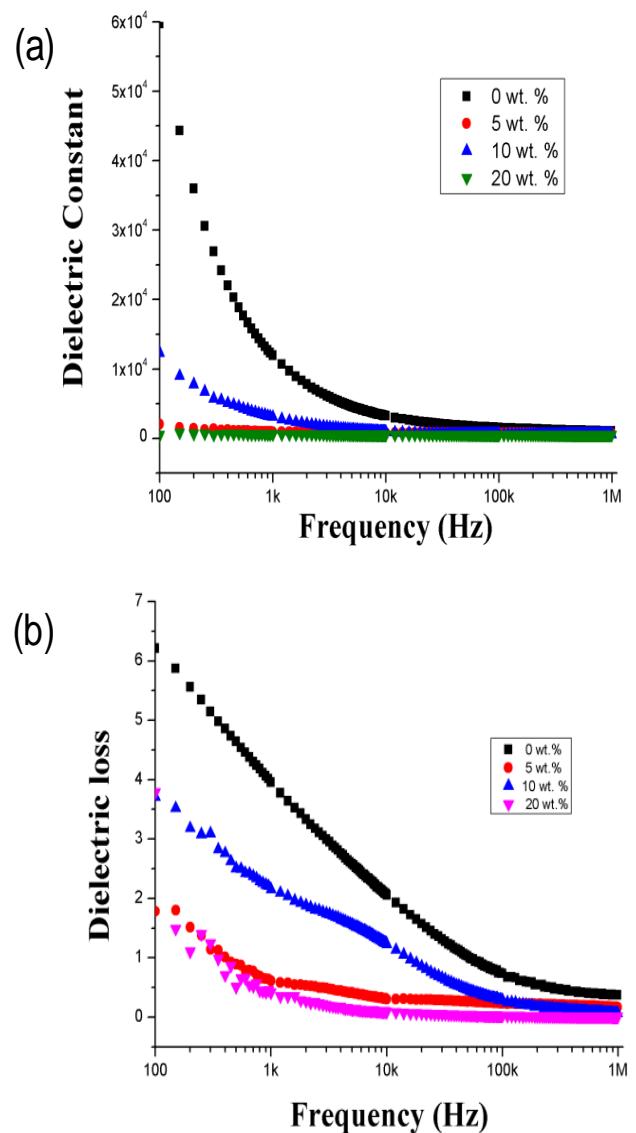
Fig. 2. XRD patterns for Li-Ni-Co ferrite/SiO<sub>2</sub> nanocomposites sintered at 1000°C for 6 hrs.

**Table 1.** Various structural parameters for Li-Ni-Co ferrite/SiO<sub>2</sub> composites.

SiO <sub>2</sub> content (wt. %)	Lattice constant a (Å)	X-ray density (gcm <sup>-3</sup> )	Experimental density (gcm <sup>-3</sup> )	Crystallite size (nm)	Grain size (nm)
0	8.329	4.873	3.309	38	1980
5	8.326	4.879	3.445	40	678
10	8.326	4.878	3.723	32	363
20	8.319	4.890	3.137	30	349

The various structural properties such as lattice constant, crystallite size and X-ray density calculated from XRD data are tabulated in **Table 1**. It is observed that the lattice constant does not change significantly with the substitution of SiO<sub>2</sub>. The diffraction peaks are observed to be broadened while the intensity decreases with the increase in SiO<sub>2</sub> concentration. The crystallite size, therefore, decreases with increase in SiO<sub>2</sub> content and found to be in the range 30 – 40 nm. The experimental density is observed to increase with the content of SiO<sub>2</sub>, reaching a maximum at 10% SiO<sub>2</sub> addition.

The morphology of the samples as depicted in **Fig. 3**, showed a decrease in the average grain size from 1980 nm to 349 nm with the increase of SiO<sub>2</sub> concentration. The pure sample with no addition of SiO<sub>2</sub>, showed an inhomogeneous distribution of the grains, the bigger grains being embedded among the finer grains ones. However, with addition of SiO<sub>2</sub>, the grain size distribution became more uniform with refined microstructures. The microstructures of the sample with x = 20 wt. % indicate the formation of liquid phase film at the grain boundaries (**Fig. 3(d)**) possibly due to the excessive amount of SiO<sub>2</sub> content. Similar observations have been reported by other researchers [12, 21].

**Fig. 3.** (a-d) SEM photograph of Li<sub>0.41</sub>Ni<sub>0.1</sub>Co<sub>0.08</sub>Fe<sub>2.41</sub>O<sub>4+x</sub>SiO<sub>2</sub> nanocomposites (a) x = 0wt. %, (b) x = 5wt. %, (c) x = 10wt. % and (d) x = 20wt. %.**Fig. 4.** Plots of (a) dielectric constant and (b) dielectric loss versus frequency for Li<sub>0.41</sub>Ni<sub>0.1</sub>Co<sub>0.08</sub>Fe<sub>2.41</sub>O<sub>4+x</sub>SiO<sub>2</sub> nanocomposites.

The variation of dielectric constant with frequency shown in **Fig. 4(a)**, showed the normal dispersive behavior, where the dielectric constant decreased abruptly with increase of frequency maintaining a nearly constant value at higher frequencies.

The dispersive behavior can be explained from Verwey mechanism of electron hopping and space charge polarization where the mechanism of dielectric polarization is taken to be similar to that of electrical conduction. According to this mechanism, the main mode of conduction is due to the hopping of electrons between ions of the same element present in more than one valency state at crystallographic equivalent lattice sites. The Fe<sup>2+</sup> ions which may have been formed from partial evaporation of lithium and oxygen at the ferrite surfaces during synthesis resides at the B-sites [23]. Therefore, the electron hopping in the present case takes place between Fe<sup>2+</sup> and Fe<sup>3+</sup> ions at the B sites. According to Koop's

two-layer model [24] in agreement with the inhomogeneous dielectric structure of Maxwell-Wagner type [25, 26], ferrites are assumed to be composed of well-conducting grains separated by poorly conducting grain boundaries. During hopping the high resistive grain boundaries block the mobile charge carriers (i.e. electrons) thus inhibiting charge migration and leading to the piling up of the charges at the grain boundaries under the influence of an electric field and hence producing space charge polarization, leading to a large value of dielectric constant. [27]. As the frequency of the applied field is increased, the charges are not able to follow the alternating field, and the polarization produced is decreased. Therefore, a decrease in dielectric constant is observed. At very high frequency, the charge oscillation become independent of the applied field and thus the dielectric constant remains nearly constant.

The frequency variation of dielectric loss for the nanocomposites is depicted in Fig. 3(b). It is seen that the loss is high at low frequency and continuously decreases with increase of frequency, remaining constant at higher frequencies. This can be understood from Koop's phenomenological model [24]. Dielectric loss is reported to be contributed by the presence of impurities and structural inhomogeneities and arises due to the lag of polarization with the applied electric field [28]. The dielectric loss is observed to be high for the pure Li-Ni-Co ferrite ( $x = 0$  wt.%) sample and found to decrease with the substitution of SiO<sub>2</sub>.

Furthermore, it can be seen from Fig. 4(a) that the dielectric constant of pure Li-Ni-Co ferrite is considerably higher than those of nanocomposites. This can be explained in terms of the small nanometric crystallites obtained due to addition of SiO<sub>2</sub>. These small crystallites contain greater number of insulating grain boundaries that act as scattering centers to the conduction of electrons, thereby restricting the exchange of electrons. Moreover, the small crystallites possess large surface to volume ratio with greater probability for converting the Fe<sup>2+</sup> ions, which may have formed during synthesis, back to Fe<sup>3+</sup> ions. Hence, the charged species available for electron exchanges are consequently restricted in the SiO<sub>2</sub> added composites. Thus, Verwey mechanism of electron hopping is decreased resulting in reduction of the dielectric constant values. Also the value of dielectric loss for the nanocomposites are found to be much reduced as compared to pure Li-Ni-Co ferrite, which may be attributed to the small nanocrystallites as explained above. Such reduction in dielectric loss is desirable for high frequency applications, since low dielectric loss values increases the depth of penetration of electromagnetic waves as well as reduces skin effect [29].

## Conclusion

Li-Ni-Co ferrite/SiO<sub>2</sub> composites with representative formula Li<sub>0.41</sub>Ni<sub>0.1</sub>Co<sub>0.08</sub>Fe<sub>2.41</sub>O<sub>4</sub>+ xSiO<sub>2</sub> (i.e.,  $x = 0$ wt. %, 5wt. %, 10wt. % and 20wt. %) were successfully prepared by sol-gel method. X-ray diffraction studies show

diffraction peaks of single phase spinel structure with peaks of SiO<sub>2</sub>. The lattice constant, crystallite size, theoretical density and average grain size were calculated. The crystallite size ranges from 30-40nm. The microstructure of the samples showed refinement of grains with the addition of SiO<sub>2</sub>, however, presence of excessive amount of SiO<sub>2</sub> leads to the formation of liquid phase. The room temperature dielectric constant and dielectric loss studied as a function of frequency showed dispersion. The nanocomposites exhibited much reduced values of dielectric constant and dielectric loss may be useful for high frequency applications.

## Acknowledgements

The authors would like to acknowledge the XRD and SEM central facilities of Manipur University.

## References

1. Smit, J.; Wijn, H. P. J.; *Philips Tech. Lib.*, **1959**, 136.
2. Argentina, G. M.; Baba, P.D. *IEEE Trans. Microw. Theory Tech.*, **1974**, 22, 652.
3. Reddy, P. V. B.; Ramesh, B.; Reddy, Ch. G.; *Physica B*, **2010**, 405, 1852.
4. Goldman, A. (Eds.); *Modern Ferrite Technology*; Springer Science and Business Media: USA, **2006**.
5. Kumar, A.; Kumar, P.; Rana, G.; Yadav, M. S.; Pant, R. P.; *Appl. Sci. Lett.*, **2015**, 2, 33.
6. Nilima, N.; Maisnam, M.; Phanjobam, S.; *Int. J. Eng. Innov. Res.*, **2015**, 4, 415.
7. Baba, P. D.; Argentina, G. M.; Courtney, W. E.; Dionne, G. F.; Temme, D. H.; *IEEE Trans. Magn.*, **1972**, 8, 83.
8. Kishan, P. *Microwave Lithium ferrites*, In *Microwave Materials*; Murthy, V.R.K.; Sundaram, S.; Viswanathan, B. (Eds.); Springer-Verlag Berlin Heidelberg: USA, **1994**.
9. Lakshmi, M.; Kumar, K. V.; Thyagarajan, K.; *Adv.Nanopar.*, **2016**, 5,103.
10. Ahmed, M. A.; Afify, H. H.; El Zawawia, I. K.; Azab, A. A.; *J. Magn. Mater.*, **2012**, 324, 2199.
11. Chakraverty, S.; Mandal, K.; Chatterjee, S.; Kumar, S.; *Indian. J. Phys.*, **2004**, 78A, 177.
12. Kotnala, R. K.; Verma, V.; Pandey, V.; Awana, V. P. S.; Aloysius, R. P.; Kothari, P. C.; *Solid Stat. Comm.*, **2007**, 143, 527.
13. Maisnam, M.; Phanjobam, S.; Sharma, H. N. K.; Thakur, O.P.; Radhapiyari, L.; Prakash, C.; *Int. J. of Mod. Phys. B*, **2003**, 17, 3881.
14. Siligardi, C.; Leonelli, C.; Bondioli, F.; Corradi, A.; PellakaCo, G. C.; *J. Eur. Ceram. Soc.*, **2000**, 20,177.
15. Giri, A. K.; de Julian, C.; Gonzalez, J. M.; *J. Appl. Phys.*, **1994**, 76, 6573.
16. Maisnam, M.; Phanjobam, S.; Sharma, H. N. K.; Prakash, C.; Radhapiyari, L.; Thakur, O. P.; *Physica B*, **2005**, 370, 1.
17. Wu, K. H.; Ting, T. H.; Yang, C. C.; Wang, G. P.; *Mater. Sci. Eng., B*, **2005**, 123, 227.
18. Perez, E.; Gomez-polo, C.; Larumbe, S.; Perez-Landazabal, J.I.; Sagredo, V.; *Rev. Mex. Fis.*, **2012**, 58, 104.
19. Mathew, L.; Narayanankutty, S. K. Abstract of Paper, Synthesis and Characterisation of Nanosilica, Conference, Adv. Polym. Tech. Conf. 279, IN, Vol. 279, **2010**.
20. Kotoky, T.; Dolui, S. K.; *J. Sol. Gel. Sci. Technol.*, **2004**, 29, 107.
21. Praveena, K.; Sadhana, K.; Murthy, S. R.; *J. Magn. Mater.*, **2011**, 323, 2122.

22. Swalka, O.; Sharma, R. K.; Sebastian, V.; Lakshmi, N.; Venugopala, K.; *J. Magn. Magn. Mater.*, **2007**, *313*, 198.
23. Koops, C. G.; *Phys. Rev.*, **1951**, *83*, 121.
24. Verwey, E. J. W.; de Boer, J. M.; *Rec. trav. Chim-Pays-Bas*, **1936**, *55*, 531.
25. Maxwell, J. C. (Eds.); *Electricity and Magnetism*; Oxford University Press: UK, **1929**.
26. Wagner, K.W.; *Ann. Phys.*, **1913**, *40*, 817.
27. Hench, L. L.; West, J. K. (Eds.); *Principles of Electronic Ceramics*; Wiley: USA, **1990**.
28. Amarendra, K. S.; Verma, A.; Thakur, O. P.; Prakash, C.; Goel, T. C.; Mendiratta, R. G.; *Mater. Lett.*, **2003**, *57*, 1040.
29. Nasir, S; Anis-ur Rehman, M.; *Phys. Scr.*, **2011**, *84*, 1.